Materials Horizons

COMMUNICATION

Systematic study of exciton diffusion length in organic semiconductors by six experimental methods†

Cite this: DOI: 10.1039/c3mh00089c

Received 21st August 2013
Accepted 9th January 2014

DOI: 10.1039/c3mh00089c

rsc.li/materials-horizons

By Jason Lin,[a] Oleksandr V. Mikhnenko,[ab] Jingrun Chen,[c] Zarifi Masri,[d] Arvydas Ruseckas,[d] Alexander Mikhailovsky,[a] Reilly P. Raab,[a] Jianhua Liu,[a] Paul W. M. Blom,[e] Maria Antonietta Loi,[b] Carlos J. García-Cervera,[c] Ifor D. W. Samuel[d] and Thuc-Quyen Nguyen*[a]

Six experimental methods have been used to investigate the exciton diffusion length in materials with systematic chemical modifications. We find that exciton diffusion length correlates with molecular ordering. We discuss situations in which certain experimental techniques are more appropriate.

Exciton diffusion plays a vital role in the function of many organic semiconducting opto-electronic devices. Exciton diffusion length (L_D) is the characteristic distance that excitons are able to diffuse during their lifetime in a given material. A short L_D limits the dissociation of excitons into free charges in planar-heterojunction organic solar cells.[1,2] Conversely, a long L_D in organic light emitting diodes (OLEDs) can limit luminous efficiency if excitons diffuse to non-radiative quenching sites such as oxidation defects,[3] electrodes,[4] and polarons.[5] Exciton diffusion has been studied in a number of small molecules[1,2,6–17] and conjugated polymers.[9,18–32] However, it remains challenging to understand the relationship between the chemical structure and the exciton diffusion length. There are only a few works which investigate exciton diffusion length as a function of chemical structure.[1,11,13,21,27,33] In particular the effect of conjugation length on the exciton diffusion has not been addressed.

Several methods have been used to measure exciton diffusion length; however, it is unclear which methods are more reliable for a given situation. Reported techniques to measure exciton diffusion length include photoluminescence (PL) surface quenching,[1,11,21,22,24–26,34–37] time-resolved PL bulk quenching modeled with a Monte Carlo simulation,[16,27] exciton–exciton annihilation,[15,23,26,29,38] modeling of solar cell photocurrent spectrum,[6,9,10,18,35,39–45] time-resolved microwave conductance,[17,46,47] spectrally resolved PL quenching,[13,33,48,49] and Förster resonance energy transfer theory.[13,33,50] Currently, there is little known on how the value of the measured exciton diffusion length of the same material can vary depending on the technique employed. Consequently, it is difficult to draw conclusions regarding the structure–property relationships across previous studies.

In this work, a thorough investigation has been performed to study the dependence of exciton diffusion length on chemical structure using six experimental techniques. We have utilized phenyl substituted diketopyrrolopyrrole (DPP) small molecules (Fig. 1) as our model system. The chemical structure has been systematically modified in regards to conjugation length and functional groups. We show that decreasing the conjugation length increases molecular ordering, which is correlated with an enhancement of exciton diffusion length.

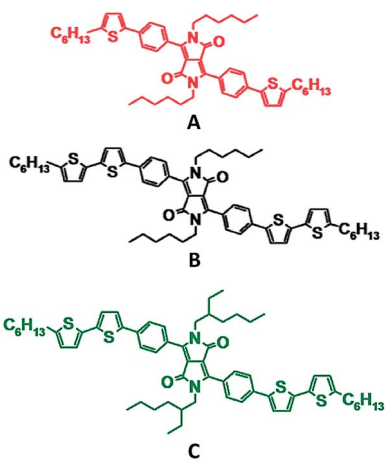

Fig. 1 Chemical structures for compounds A, B, and C.

[a]Center for Polymers and Organic Solids, Department of Chemistry and Biochemistry, University of California, Santa Barbara, CA 93106, USA. E-mail: quyen@chem.ucsb.edu; Fax: +1 805 893 4120; Tel: +1 805 893 4851

[b]Zernike Institute for Advanced Materials, University of Groningen, Nijenborgh 4, 9747 AG Groningen, The Netherlands. E-mail: m.a.loi@rug.nl; Tel: +31 50 363 4119

[c]Department of Mathematics, University of California at Santa Barbara, Santa Barbara, CA, 93106, USA. E-mail: cgarcia@math.ucsb.edu; Fax: +1 805 893 2385; Tel: +1 805 893 3681

[d]Organic Semiconductor Centre, SUPA, School of Physics and Astronomy, University of St. Andrews, St Andrews, KY169SS, UK. E-mail: idws@st-andrews.ac.uk; Tel: +44 (0) 1334 46 3114

[e]Max Planck Institute for Polymer Research, Ackermannweg 10, 55128 Mainz, Germany. E-mail: blom@mpip-mainz.mpg.de; Tel: +49 6131 379-121

† Electronic supplementary information (ESI) available. See DOI: 10.1039/c3mh00089c

In general, a diffusion length is defined as the root mean squared displacement of a particle from its initial position during time τ (ref. 51):

$$L_D = \sqrt{\frac{\sum dL_i^2}{N}} = \sqrt{2ZD\tau}, \quad (1)$$

where dL_i is the displacement of a particle i from its original position and N is the total number of excitons. In the case of one-, two-, or three-dimensional diffusion, Z is equal to 1, 2, or 3, respectively.[51] However, in context of exciton diffusion a $\sqrt{2}$ factor is often omitted in eqn (1) and the values of L_D are often reported for the one-dimensional case:

$$L_D = \sqrt{D\tau}. \quad (2)$$

To be consistent with literature, we use eqn (2) in this work to define the exciton diffusion length.

Fig. 1 shows the chemical structures of the compounds that were used in this work. When going from compound A to B the conjugation length is increased by two thiophene units. Comparing B to C highlights the impact of the functional group by the replacement of the linear alkyl chains on the lactam nitrogen units with ethyl–hexyl groups. These variations in chemical structures have been shown to induce different molecular packing and film morphology,[52] which may impact the exciton diffusion length.

To understand how the experimental technique influences the resulting value of the exciton diffusion length we have used six methods to independently measure the exciton diffusion length for compounds shown in Fig. 1. The exciton diffusion length was measured using steady-state PL surface quenching (SS-SQ), time-resolved PL surface quenching (TR-SQ), exciton–exciton annihilation (EEA), time-resolved PL bulk quenching modeled with a Monte Carlo simulation (BQ-MC), time-resolved PL bulk quenching fitted with the Stern–Volmer equation (BQ-SV), and estimated using Förster resonant energy transfer (FRET) theory.

In the surface quenching techniques – such as SS-SQ and TR-SQ – steady-state or time-resolved PL is measured to determine the exciton quenching efficiency in bilayer films as a function of organic semiconductor thicknesses with a thin quenching layer. The exciton diffusion length is correlated to the maximum thickness of the material at which the majority of generated excitons can reach the quenching interface. In the EEA technique, time-resolved PL is measured at variable excitation fluence to detect the decay of excitons due to the diffusion limited collision and annihilation. The exciton diffusion length is correlated to the exciton density at which the majority of generated excitons can be quenched *via* EEA. In the bulk (or volume) quenching techniques, organic semiconductor is mixed with exciton quenching molecules to form homogeneous blends. Exciton quenching efficiency in blend films is measured as a function of quencher concentration. The quenching can be analysed by a Monte Carlo simulation or the Stern–Volmer equation leading to exciton diffusion parameters. In the BQ-MC technique, the experimentally measured exciton lifetime in pristine material is inputted into the Monte Carlo simulation where the diffusion coefficient is fitted to match the experimentally measured quenching efficiency at a given PCBM concentration. In this technique, the exciton diffusion length is correlated to the distance an exciton required to travel to reach a quencher molecule. The BQ-MC and BQ-SV are similar in regards to film fabrication and measurement. In contrast to BQ-MC, BQ-SV method can be only applied to materials that show monoexponential PL decay dynamics. However, the analysis in the BQ-SV technique does not require the Monte Carlo simulation software. For the FRET theory method, the diffusion coefficient is estimated from the Förster radius and the distance between chromophores. Then the exciton diffusion length is calculated using formula (2). In the following, we will only briefly discuss the key differences between the techniques. Further details regarding the sample preparation, measurement, data analysis, and assumptions for each technique can be found in the ESI.†

In regards to sample preparation, surface quenching techniques are the most time consuming due to high demands for the sample quality. An efficient exciton quencher is required that can form a stable and sharp interface with the organic semiconductor, which is non-trivial as discussed in the ESI.† Relatively large number of samples is required (10–20) with variable thickness of organic semiconductor in the range of typically 5–50 nm. In addition a precise thickness measurement is necessary using atomic force microscopy and/or spectroscopic ellipsometry. Surface quenching techniques also assume consistent morphologies across thick and thin films. This is likely not the case for semi-crystalline materials. Samples for the bulk quenching techniques – such as BQ-MC and BQ-SV – are relatively simple to prepare since the aforementioned requirements for the film thickness, surface roughness, and interface effects do not apply. However, a good quenching agent must be available, which would homogeneously mix with the organic semiconductor. Fortunately, [6,6]-phenyl-C_{61}-butyric acid methyl ester (PCBM) can be used as such an agent in most of the cases. The bulk quenching techniques require a smaller number of samples, typically only 8 spin-coated films. These methods account for clustering of the quenchers and cannot be used if the miscibility with the quenching agent is poor. And finally, the EEA and FRET theory techniques have the simplest fabrication procedures since all measurements are done on a pristine film.

When it comes to the experimental measurements, the steady-state techniques – such as SS-SQ – are the most challenging because they require careful estimation of the amount of light absorbed and emitted.[24] Therefore, the time-resolved techniques – such as TR-SQ, BQ-MC, BQ-SV, and EEA – are preferred over the steady-state measurements. However, the time-resolved techniques usually require expensive equipment, such as ultra-fast pulsed lasers and sophisticated detectors. Thickness measurements with very high precision must be conducted for surface quenching methods that is time and resource consuming. The EEA technique requires high intensities of the pulsed lasers and good photostability of a material under study.

The data analysis procedure for the different techniques studied here range from advanced modeling and simulation to relatively simple fitting to an equation. The data modeling for the surface quenching techniques can be either simple or extensive, depending on the materials. The most complex situation occurs in the bi-layer method if the organic semiconductor and the exciton quencher have both significantly different refractive indexes and strong Förster coupling (Section 1 of ESI†). Otherwise, the exciton diffusion can be modeled with a simple analytical formula.[22] The data of the EEA technique can be modeled using an analytical model; however, the annihilation radius has to be determined using additional experiments.[26] Modeling for the bulk quenching techniques – such as BQ-MC – is not straightforward in general. However, a free software package is available for use [http://mikhnenko.com/eDiffusion]. If the bulk quenching data shows mono-exponential PL decay then analysis can be readily performed by fitting to the Stern–Volmer formula as in the BQ-SV method. Finally, FRET theory provides a relatively easy way to estimate the exciton diffusion coefficient since no fitting or modeling software is needed. However, this technique requires knowledge of a number of parameters which are often difficult to measure experimentally such as the average dipole orientation, intermolecular distance, and index of refraction (Section 5 of ESI†). In general, this is an indirect method and it must be used with caution.

Table 1 summarizes the sample preparation, measurement, and analysis in the techniques employed in this work. It shows that surface quenching techniques such as SS-SQ and TR-SQ require a large number of samples, measurements, and modeling in comparison to bulk quenching techniques such as EEA, BQ-MC, and BQ-SV.

Table 2 and Fig. 2 summarize the measurements of the exciton diffusion coefficient and exciton diffusion length. Very good agreement between different techniques is obtained in the compound C, whereas in compounds A and B the technique based on exciton–exciton annihilation gives a higher exciton diffusion coefficient than the techniques based on the bulk quenching and surface quenching.

In this series of compounds we find that the diffusion coefficient is significantly increased by decreasing the conjugation length and slightly enhanced by decreasing the molecular bulkiness of solubilizing groups. Compound A has the shortest conjugation length and shows the largest diffusion coefficient around 1×10^{-3} cm^2 s^{-1} with exciton diffusion length of 13 nm. In comparison, compounds B and C yield similar diffusion coefficients around 0.4×10^{-3} cm^2 s^{-1} and an exciton diffusion length of 9 and 8 nm, respectively. When comparing B and C within the same technique a general trend shows that the exciton diffusion coefficient and length for B is either equal or slightly greater than that of C.

The variance in diffusion coefficients between compounds A, B, and C can be due to different degrees of molecular ordering in the thin films. Previous works have shown that a greater degree of molecular ordering can enhance the exciton diffusion coefficient.[11,33,53,54]

Table 1 Sample preparation, measurement, and data analysis for various techniques to measure exciton diffusion length

Technique	Abbrev.	Sample preparation	Measurement	Data analysis	Best for
Steady-state surface quenching	SS-SQ	• 10 Pristine films with varying organic semiconductor thickness • 10 Bilayer films with a quenching layer and varying organic semiconductor thickness	• Steady-state PL spectrum as a function of thickness • Thickness • Optical constants	• Calculate quenching efficiency • Model optical constants, electrical field, generation rate, and exciton density • Fit for exciton diffusion length	Amorphous smooth films. Good quenching interface is required
Time-resolved surface quenching	TR-SQ		• Time-resolved PL decay as a function of thickness • Thickness • Optical constants		
Exciton–exciton annihilation	EEA	3–5 Pristine films	• Time-resolved PL at different excitation densities • Film density	• PL decay fitting with an analytical model	Amorphous materials
Bulk quenching with Monte Carlo modeling	BQ-MC	8–10 Blend films with varying concentrations of quencher	• Time-resolved PL decay • Film density	• Calculate quenching efficiency • Use model PL Monte Carlo simulation to	Moderately crystalline or amorphous materials
Bulk quenching with Stern–Volmer modeling	BQ-SV			• Calculate quenching efficiency • Use analytical model to fit the data	
FRET theory		3–5 Pristine films	• Steady-state absorption and PL spectrum • PL quantum yield • Film density • Thickness • Index of refraction	• Estimate distance between molecules • Calculate Förster radius and diffusion coefficient	Materials with very small quantities available

Table 2 Exciton diffusion lengths for compounds A, B, and C measured with different techniques

	Diffusion coefficient $\times 10^{-3}$ ($cm^2\ s^{-1}$)			Exciton diffusion length (nm)		
Technique	A	B	C	A	B	C
SS-SQ	1.13 ± 0.1	0.4 ± 0.07	0.36 ± 0.04	13.2 ± 0.1	9.32 ± 0.3	8.49 ± 0.16
TR-SQ	1.06 ± 0.18	0.6 ± 0.1	0.27 ± 0.03	12.7 ± 1.1	9.3 ± 0.3	7.22 ± 0.36
EEA	1.5 ± 0.4	1.5 ± 0.4	0.4 ± 0.1	14.5 ± 2.2	14.5 ± 2.2	8.4 ± 1.3
BQ-MC	0.94 ± 0.27	0.39 ± 0.13	0.4 ± 0.06	12.9 ± 1.9	9.2 ± 1.5	7.4 ± 0.6
BQ-SV	0.9 ± 0.14	0.27 ± 0.02	0.34 ± 0.02	11.4 ± 1.8	7.79 ± 0.04	6.9 ± 0.3
FRET theory	1.53 ± 0.97	0.64 ± 0.45	0.22 ± 0.12	13.8 ± 4.7	8.5 ± 3.6	5.8 ± 1.2

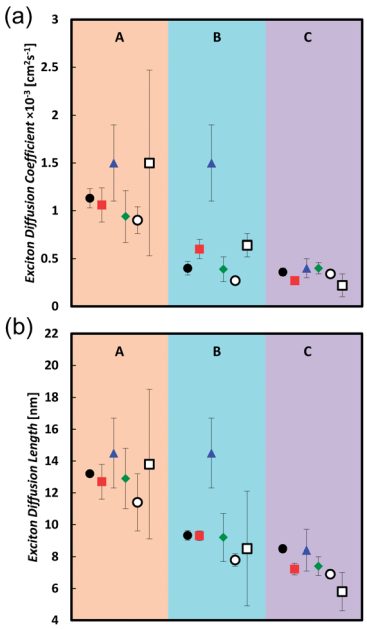

Fig. 2 Diffusion coefficients (a) and Exciton diffusion lengths (b) for compounds A, B, and C measured with SS-SQ (black circle), TR-SQ (red square), EEA (blue triangle), BQ-MC (green diamond), BQ-SV (open circle), and FRET Theory (open square).

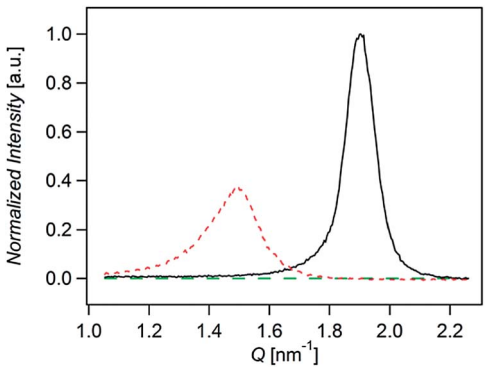

Fig. 3 X-ray diffraction for films of A (solid black line), B (dotted red line), and C (dashed green line). Scattering intensity was normalized by film thickness, structure factor, multiplicity, unit cell volume, and the Lorenz-polarization.

Fig. 3 shows the normalized X-rays scattering intensity *versus* scattering vector $\boldsymbol{Q}$ for thin films of compounds A, B, and C. The normalization accounts for film thickness, structure factor, multiplicity, unit cell volume, and the Lorenz-polarization factor (Section 6 in ESI†). We also took into account the orientation of the crystallites by measuring the angular distribution of the scattered (Fig. S12 ESI†). Integration of peaks areas in Fig. 3 shows that the relative crystallinity of A is roughly 1.6 times greater than B. Compound C does not show any scattering.

Therefore the relative crystallinity follows A > B > C, which is similar to the trend we observe in the diffusion coefficients. In this way we find that the diffusion coefficient correlates with the relative crystallinity.

In regards to the measurement of exciton diffusion length it is important to consider the degree of anisotropy in films. For instance, anthracene single crystals show L_D = 36, 60, and 100 nm in the *c*, *a*, and *b* crystalline directions respectively.[55] In our analysis of the angular distribution of the scattered intensity (Fig. S10 ESI†) we found that crystallites in films of A and B are textured out of plane and therefore anisotropic. While our x-ray diffraction measurements confirm the presence of anisotropy, it does not quantify degree of anisotropy since the volume fraction of amorphous and crystalline regions is not known.

To probe anisotropy in both crystalline and amorphous regions we utilized spectroscopic ellipsometry. Spectroscopic ellipsometry can be used to model the magnitude of absorption for in and out of plane direction which is correlated to the average dipole orientation of molecules in film. We find that there is no detectable anisotropy in films A, B, and C (Section 7 in ESI†). This result suggests that the volume fraction of crystallites in films of A and B is small relative to the volume fraction of the amorphous phase.

A predominantly isotropic medium in films of A, B, and C is further supported by the following observations. The exciton diffusion length in the direction out of plane is probed by the surface quenching techniques. We found that the obtained value is very similar to the exciton diffusion length probed in three dimensions using the bulk quenching techniques. Moreover, all three materials make homogeneous mixture with PCBM molecules for PCBM concentrations of 10^{17}–10^{18} cm^{-3} (Fig. S7†). This concentration range corresponds to the average distance between PCBM molecules of 10–20 nm. Thus the crystallites (if present) must be smaller than this distance that corresponds to the length-scale of exciton diffusion. Therefore materials A, B, and C can be considered isotropic on the scale of exciton diffusion length.

The correlation between relative crystallinity of the films with exciton diffusion length can be rationalized using the consideration that the Förster energy transfer facilitates singlet exciton diffusion in organic semiconductors. The efficiency of the FRET is rapidly decreasing with the distance between the chromophores. Therefore materials with shorter intermolecular distances are expected to have higher exciton diffusion coefficient, for similar Förster radii. Although it is difficult to estimate the intermolecular distance in mostly amorphous materials, it is likely that materials with higher affinity to form crystallites pack more densely on average. Indeed, our champion material A exhibits the highest affinity to form crystallites resulting in the largest diffusion coefficient in the series. While materials B and C show weaker affinity to form crystallites and thus lower diffusion coefficient.

From a practical stance, it is useful to investigate how the measured exciton diffusion length of a single material varies depending on the measurement technique employed. Consistent result across different techniques is achieved in the amorphous material C. In contrast, the EEA technique gives greater diffusion coefficients for compounds A and B which is attributed to exciton migration to crystalline regions where exciton–exciton collision and annihilation is enhanced. This result shows that caution should be taken when comparing exciton diffusion lengths of semi-crystalline materials measured by different techniques.

In this work we have covered six techniques to measure the exciton diffusion length. We find that certain techniques are more appropriate given the material properties along with the instrumentation and analysis software available. We find that the BQ-MC technique to be ideal for the measurement of exciton diffusion length for a broad range of materials due to its facile sample fabrication along with its minimal assumptions in modeling. However, BQ-MC does require an organic semiconductor which is miscible with PCBM, instrumentation for time-resolved spectroscopy, and simulation software. When the organic semiconductor exhibits mono-exponential decay the BQ-SV technique can be used which does not require simulation software. The EEA and FRET Theory techniques are better suited for organic semiconductors, which have poor miscibility with PCBM and are highly crystalline, since the measurements are performed on pristine films. The EEA technique is also advantageous in situations when an efficient quencher is not available. In general, surface quenching techniques such as SS-SQ and TR-SQ are the most demanding in regards to sample fabrication, measurement, and analysis. However, surface quenching techniques directly measure exciton diffusion length and can be accurately employed when the organic semiconductor and the exciton quencher are able to form a sharp and efficient quenching interface.

Conclusions

In summary, we have compared and contrasted six techniques to measure exciton diffusion length. Very good agreement between different techniques is obtained in amorphous films, whereas in semi-crystalline films the technique based on exciton–exciton annihilation gives a higher exciton diffusion coefficient and subsequently larger diffusion length than the techniques based exciton quenching. All the approaches are useful and the combined results give insight into structure–property relations for exciton diffusion. Different techniques have different advantages and disadvantages, and we discussed key differences in fabrication, measurement, and analysis. Consistent results are obtained with surface and with bulk quenching techniques, which indicates that diffusion in the direction perpendicular to the plane of the film and 3D diffusion in the bulk are not different, and hence isotropic. We find that bulk quenching techniques are convenient for systematic studies of exciton diffusion length since the sample preparation procedure is quite simple and fast and the analysis can be done using an open source Monte-Carlo software or fitting to the Stern–Volmer equation. We investigated the dependence of exciton diffusion length on systematic chemical modifications. It is shown that decreasing the conjugation length of compound B to form compound A results in an enhancement in the exciton diffusion coefficient from 0.4×10^{-3} cm^2 s^{-1} to 1×10^{-3} cm^2 s^{-1} and exciton diffusion length from 9 nm to 13 nm. We attribute this to an increase in relative molecular ordering upon decreasing the conjugation length. It is also shown that decreasing the molecular bulkiness by replacement of the ethyl–hexyl groups by the linear alkyl chains has little effect on the resulting exciton diffusion parameters.

Acknowledgements

The authors thank the National Science Foundation (NSF) Division of Materials Research, NSF-SOLAR for the financial support. TQN thanks the Camille Dreyfus Teacher Scholar Award and the Alfred Sloan Research Fellowship program. Z.M. is grateful to the Government of Brunei Darussalam for financial support. Work at St Andrews is supported by the Engineering and Physical Sciences Research Council of the UK and by the European Research Council of the European Union. We thank Alex Sharenko for useful discussion.

Notes and references

1 Y. Terao, H. Sasabe and C. Adachi, *Appl. Phys. Lett.*, 2007, **90**, 103515.
2 S. M. Menke, W. A. Luhman and R. J. Holmes, *Nat. Mater.*, 2013, **12**, 152–157.
3 H. Antoniadis, L. J. Rothberg, F. Papadimitrakopoulos, M. Yan, M. E. Galvin and M. A. Abkowitz, *Phys. Rev. B: Condens. Matter Mater. Phys.*, 1994, **50**, 14911–14915.
4 A. L. Burin and M. A. Ratner, *J. Phys. Chem. A*, 2000, **104**, 4704–4710.
5 E. J. W. List, C. H. Kim, W. Graupner, G. Leising and J. Shinar, *Mater. Sci. Eng., B*, 2001, **85**, 218–223.
6 D. Qin, P. Gu, R. S. Dhar, S. G. Razavipour and D. Ban, *Phys. Status Solidi A*, 2011, **208**, 1967–1971.
7 O. V. Mikhnenko, R. Ruiter, P. W. M. Blom and M. A. Loi, *Phys. Rev. Lett.*, 2012, **108**, 137401.

8 B. A. Gregg, J. Sprague and M. W. Peterson, *J. Phys. Chem. B*, 1997, **101**, 5362–5369.
9 T. Stübinger and W. Brütting, *J. Appl. Phys.*, 2001, **90**, 3632–3641.
10 C. L. Yang, Z. K. Tang, W. K. Ge, J. N. Wang, Z. L. Zhang and X. Y. Jian, *Appl. Phys. Lett.*, 2003, **83**, 1737–1739.
11 S.-B. Rim, R. F. Fink, J. C. Schöneboom, P. Erk and P. Peumans, *Appl. Phys. Lett.*, 2007, **91**, 173504.
12 A. Holzhey, C. Uhrich, E. Brier, E. Reinhold, P. Bäuerle, K. Leo and M. Hoffmann, *J. Appl. Phys.*, 2008, **104**, 064510.
13 R. R. Lunt, N. C. Giebink, A. A. Belak, J. B. Benziger and S. R. Forrest, *J. Appl. Phys.*, 2009, **105**, 053711.
14 H. Gommans, S. Schols, A. Kadashchuk, P. Heremans and S. C. J. Meskers, *J. Phys. Chem. C*, 2009, **113**, 2974–2979.
15 S. Cook, A. Furube, R. Katoh and L. Han, *Chem. Phys. Lett.*, 2009, **478**, 33–36.
16 O. Mikhnenko, J. Lin, Y. Shu, J. E. Anthony, P. W. M. Blom, T.-Q. Nguyen and M. A. Loi, *Phys. Chem. Chem. Phys.*, 2012, **14**, 14196–14201.
17 M. C. Fravventura, J. Hwang, J. W. A. Suijkerbuijk, P. Erk, L. D. A. Siebbeles and T. J. Savenije, *J. Phys. Chem. Lett.*, 2012, **3**, 2367–2373.
18 J. J. M. Halls, K. Pichler, R. H. Friend, S. C. Moratti and A. B. Holmes, *Appl. Phys. Lett.*, 1996, **68**, 3120–3122.
19 A. Haugeneder, M. Neges, C. Kallinger, W. Spirkl, U. Lemmer, J. Feldmann, U. Scherf, E. Harth, A. Gügel and K. Müllen, *Phys. Rev. B: Condens. Matter Mater. Phys.*, 1999, **59**, 15346–15351.
20 D. E. Markov, J. C. Hummelen, P. W. M. Blom and A. B. Sieval, *Phys. Rev. B: Condens. Matter Mater. Phys.*, 2005, **72**, 045216.
21 D. E. Markov, C. Tanase, P. W. M. Blom and J. Wildeman, *Phys. Rev. B: Condens. Matter Mater. Phys.*, 2005, **72**, 045217.
22 D. E. Markov, E. Amsterdam, P. W. M. Blom, A. B. Sieval and J. C. Hummelen, *J. Phys. Chem. A*, 2005, **109**, 5266–5274.
23 A. J. Lewis, A. Ruseckas, O. P. M. Gaudin, G. R. Webster, P. L. Burn and I. D. W. Samuel, *Org. Electron.*, 2006, **7**, 452–456.
24 S. R. Scully and M. D. McGehee, *J. Appl. Phys.*, 2006, **100**, 034907.
25 C. Goh, S. R. Scully and M. D. McGehee, *J. Appl. Phys.*, 2007, **101**, 114503.
26 P. E. Shaw, A. Ruseckas and I. D. W. Samuel, *Adv. Mater.*, 2008, **20**, 3516–3520.
27 O. V. Mikhnenko, H. Azimi, M. Scharber, M. Morana, P. W. M. Blom and M. A. Loi, *Energy Environ. Sci.*, 2012, **5**, 6960–6965.
28 A. J. Ward, A. Ruseckas and I. D. W. Samuel, *J. Phys. Chem. C*, 2012, **116**, 23931–23937.
29 Z. Masri, A. Ruseckas, E. V. Emelianova, L. Wang, A. K. Bansal, A. Matheson, H. T. Lemke, M. M. Nielsen, H. Nguyen, O. Coulembier, P. Dubois, D. Beljonne and I. D. W. Samuel, *Adv. Energy Mater.*, 2013.
30 E. Hennebicq, G. Pourtois, G. D. Scholes, L. M. Herz, D. M. Russell, C. Silva, S. Setayesh, A. C. Grimsdale, K. Müllen, J.-L. Brédas and D. Beljonne, *J. Am. Chem. Soc.*, 2005, **127**, 4744–4762.
31 X. Zhang, Z. Li and G. Lu, *Phys. Rev. B: Condens. Matter Mater. Phys.*, 2011, **84**, 235208.
32 S. Athanasopoulos, E. V. Emelianova, A. B. Walker and D. Beljonne, *Phys. Rev. B: Condens. Matter Mater. Phys.*, 2009, **80**, 195209.
33 R. R. Lunt, J. B. Benziger and S. R. Forrest, *Adv. Mater.*, 2010, **22**, 1233–1236.
34 Y. Wu, Y. C. Zhou, H. R. Wu, Y. Q. Zhan, J. Zhou, S. T. Zhang, J. M. Zhao, Z. J. Wang, X. M. Ding and X. Y. Hou, *Appl. Phys. Lett.*, 2005, **87**, 044104.
35 M. Theander, A. Yartsev, D. Zigmantas, V. Sundström, W. Mammo, M. R. Andersson and O. Inganäs, *Phys. Rev. B: Condens. Matter Mater. Phys.*, 2000, **61**, 12957.
36 Y. C. Zhou, Y. Wu, L. L. Ma, J. Zhou, X. M. Ding and X. Y. Hou, *J. Appl. Phys.*, 2006, **100**, 023712.
37 O. V. Mikhnenko, F. Cordella, A. B. Sieval, J. C. Hummelen, P. W. M. Blom and M. A. Loi, *J. Phys. Chem. B*, 2008, **112**, 11601–11604.
38 P. E. Shaw, A. Ruseckas, J. Peet, G. C. Bazan and I. D. W. Samuel, *Adv. Funct. Mater.*, 2010, **20**, 155–161.
39 A. K. Ghosh and T. Feng, *J. Appl. Phys.*, 1978, **49**, 5982–5989.
40 J. Wagner, T. Fritz and H. Böttcher, *Phys. Status Solidi A*, 1993, **136**, 423–432.
41 V. Bulović and S. R. Forrest, *Chem. Phys. Lett.*, 1995, **238**, 88–92.
42 L. A. A. Pettersson, L. S. Roman and O. Inganäs, *J. Appl. Phys.*, 1999, **86**, 487.
43 P. Peumans, A. Yakimov and S. R. Forrest, *J. Appl. Phys.*, 2003, **93**, 3693.
44 S.-B. Rim and P. Peumans, *J. Appl. Phys.*, 2008, **103**, 124515.
45 A. Huijser, T. J. Savenije, A. Shalav and L. D. A. Siebbeles, *J. Appl. Phys.*, 2008, **104**, 034505.
46 T. J. Savenije and L. D. Siebbeles, in *Laser Science, Optical Society of America*, 2010, p. LWC5.
47 J. E. Kroeze, T. J. Savenije, M. J. W. Vermeulen and J. M. Warman, *J. Phys. Chem. B*, 2003, **107**, 7696–7705.
48 K. J. Bergemann and S. R. Forrest, *Appl. Phys. Lett.*, 2011, **99**, 243303.
49 B. P. Rand, D. Cheyns, K. Vasseur, N. C. Giebink, S. Mothy, Y. Yi, V. Coropceanu, D. Beljonne, J. Cornil, J.-L. Brédas and J. Genoe, *Adv. Funct. Mater.*, 2012, **22**, 2987–2995.
50 T. K. Mullenbach, K. A. McGarry, W. A. Luhman, C. J. Douglas and R. J. Holmes, *Adv. Mater.*, 2013, **25**, 3689–3693.
51 M. Pope and C. E. Swenberg, *Electronic processes in organic crystals and polymers*, Oxford University Press, 1999.
52 C. Kim, J. Liu, J. Lin, A. B. Tamayo, B. Walker, G. Wu and T.-Q. Nguyen, *Chem. Mater.*, 2012, **24**, 1699–1709.
53 L. D. A. Siebbeles, A. Huijser and T. J. Savenije, *J. Mater. Chem.*, 2009, **19**, 6067–6072.
54 G. Wei, R. R. Lunt, K. Sun, S. Wang, M. E. Thompson and S. R. Forrest, *Nano Lett.*, 2010, **10**, 3555–3559.
55 R. C. Powell and Z. G. Soos, *J. Lumin.*, 1975, **11**, 1–45.